Process Modeling of Flexible Robotic Grinding

Jianjun Wang*, Yunquan Sun*, zhongxue Gan*, and Kazem Kazerounian **

* Robotic & Automation, ABB Corporate Research, USA
(Tel : +1-860-285-6964; E-mail: jianjun.wang@us.abb.com)
**Department of Mechanical Engineering, University of Connecticut, CT, USA
(Tel : +1-860-486-2251; E-mail: kazem@engr.uconn.edu)

Abstract: In this paper, an extended process model is proposed for the application of flexible belt grinding equipment as utilized in robotic grinding. The analytical and experimental results corresponding to grinding force, material removal rate (MRR) and contact area in the robotic grinding shows the difference between the conventional grinding and the flexible robotic grinding. The process model representing the relationship between the material removal and the normal force acting at the contact area has been applied to robotic programming and control. The application of the developed model in blade grinding demonstrates the effectiveness of proposed process model.

Keywords: process modeling, robotic grinding, blade, material removal rate

1. INTRODUCTION

The contoured parts that are commonly finished using multiple axes milling machines, profilers, or by hand-held methods can also be finished using a robot along with belt grinding equipment. Owing to the higher flexibility of the robotic belt grinding workcell, this configuration offers greater versatility when dealing with many fabricated parts having irregular contoured shapes. Compared with conventional grinding processes, robotic belt grinding is more forgiving, cost effective, and introduces more versatility into many grinding and finishing operations. Depending on the application, the robotic belt grinding can be used either to achieve relatively high material removal rates and/or satisfactory surface finishes.

At present, robots are commonly employed in many conventional metal-grinding applications. However, unlike the conventional grinding process in which the grinding wheels used are relatively rigid, the abrasive element in robotic belt grinding is far more flexible. Therefore the conventional grinding process modeling cannot directly be applied. Since the use of flexible belt grinding equipment in manufacturing applications is relatively recent, currently there is a negligible amount of published information available in this field. Thus, the primary objective of this study is to develop a process model suitable for the application of flexible belt grinding equipment as utilized in robotic material grinding applications.

2. NOMENCLATURE

a	Depth of cut, mm
A_c	Contact area between the grinding wheel and workpiece, mm^2/mm
F_{th}	Threshold force to removal the material from workpiece, N/mm^2
WRP	Material removal parameter, mm^3/s, N
MRR	Material removal rate, mm^3/s, mm
F_n	Normal force, N/mm
R	Contact wheel radius, mm
L	Contact length, mm
θ	Contact angle, degree
Δ	Contact wheel deformation, mm
V	Workpiece infeed rate, mm/s
C_r	Robot compliance, mm/N
C_w	Grinding compliance, mm/N
C_t	Equivalent tooling compliance, mm/N
C_g	Grinding loop compliance, mm/N
ΔX_r	Robot deformation, mm
ΔX_t	Tool wear, mm
ΔX_g	Grinder displacement, mm
ε	Deformation coefficient

3. OVERVIEW OF GRINDING PROCESS MODELING

Many researchers and engineers have made a great effort to develop the process modeling for grinding process. Hahn [1] described the conventional grinding process by the "Wheelwork Characteristic Chart" using the relationship between the volumetric rates of stock removal and the normal interface force intensity. It was shown that the sharpness of the grinding wheel will be decreased as wear flat develops on the abrasive grains.

When robotic grinding was emerged, researchers have tried to apply conventional grinding process model to flexible robotic grinding. Most previous work has been done in robotic deburring or disk grinding [2]. A static model [3] and dynamic model [4] for robotic disk grinding system were established by Whitney and Brown. In those conventional models, workpiece cutting stiffness and grinding wheel wear stiffness are simply defined as a constant $K_w = F/dx$ and $K_s = F/ds$. Persoons and Vanherck [5] built a model based on experimental results for robotic cup wheel grinding. Persoons's model confirmed the well-known behavior in conventional grinding that the workpiece material removal rate is proportional to the exerted force.

All of the previous models are based on the assumption that the contact area between the workpiece and grinding wheel is simple-point-contact. As a result, the contact area is treated as constant and process modeling is a simplified relationship between the normal force and the material removal rate.

In robotic belt grinding, the contact area between the abrasive surface and workpiece varies, and as a consequence, the grinding force always varies in the grinding process even though the depth of cut is a constant. Literature searches have not identified any information regarding the compliant nature of the belt grinding process. The preliminary test results conducted in this research have identified significant differences between robotic belt grinding and conventional grinding.

Therefore, it is necessary for robotic industry to develop the process modeling to adapt into flexible robotic grinding. Based on the study of the material removal mechanism and the dynamic characteristics of the associated robot, process characterization will be investigated in an attempt to obtain appropriate process input-output relationships. This part of the study will establish the basic process modeling for a flexible belt grinding process from both analytical and experimental results.

4. THEORETICAL ANALYSIS OF ROBOTIC GRINDING PROCESS MODEL

4.1 Basic process model in robotic grinding

In order to effectively investigate the new process model, the basic concepts set forth by Hahn and Lindsay will be pursued in this study. However, further considerations that must be addressed are summarized as:

1) In conventional grinding, flat or cylindrical, the applied equivalent diameters are in most times considered to be constant. However, a belt grinding process is more commonly applied to parts having irregular contours and local curvature must be considered. The real area of contact is far more complicated than in conventional grinding. It is not only related to the development of wear flats on the abrasive grains, but also related to the other important parameters such as the local curvature of the workpiece, contact wheel hardness and diameter, belt tension, belt properties.
2) The surface speed of the grinding wheel is an important parameter in the conventional grinding process. Because of the variation of belt grinding contact area during the grinding process, the workpiece infeed rate must be controlled in an effort to maintain a more or less constant rate of material removal.
3) Because of the relative flexibility of belt grinding elements, it is anticipated that the threshold force behavior is considerably different from that of conventional grinding.

Considering those factors, this study will focus on the relationship among the normal cutting force, the MRR and the contact area, which can be described by the following equation:

$$A_c \cdot F_{th} + MRR / WRP = F_n \quad (1)$$

Where:

- A_c Contact area between the grinding wheel and workpiece, mm^2/mm;
- F_{th} Threshold force to removal the material from workpiece, N/mm^2;
- WRP Material removal parameter ($mm^3/s, N$), which is the material removal rate under unit force;
- MRR Material removal rate ($mm^3/s, mm$);
- F_n Normal force, N/mm.

Rewriting Eq. (1) as:

$$MRR/[WRP \times A_c] + F_{th} = F_n / A_c \quad (2)$$

This rewriting indicates the following facts:

1) While the contact area changes significantly during the grinding process, contact area becomes a variable in process model. Therefore, the process model is a 3D relationship among force, MRR and contact area.
2) When the contact area is considered, the robotic grinding process is not constant force control, but constant pressure control.
3) Considering force, MRR and contact area as three variables, F_{th} and WRP determined by abrasive tool will be treated as the model parameters to be determined.

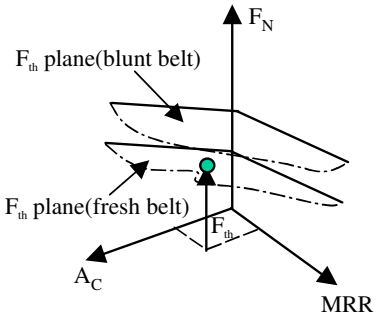

Fig. 1 Relationship among MRR, Contact Force, F_N and Contact Area, A_C under Different Belt Conditions

Fig. 1 shows the comparative relationships of F_N, MRR, and A_C, based on Eq. (1) for fresh and blunt grinding belts. Consistent with the result from Hahn, it can be seen that a force can be supported between a grinding wheel and workpiece without material removal taking place. This region is known as the "rubbing zone". When the force exceeds a critical value, material removal takes place, initially non-linearly known as the "plowing zone". As the force is increased further the removal rate increases linearly in the region known as the "cutting zone". A two dimensional model by taking a section parallel to the plan consisting of F_N and MRR axes show in Fig. 1 will be identical to the model developed by Hahn [1]. In addition, this 3D model considers the nature of the robotic grinding with flexible contact wheel and different curvature of the workpiece.

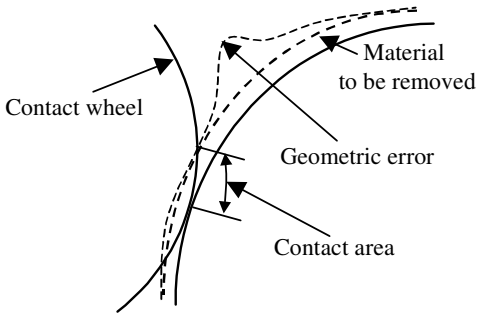

Fig. 2 Effect of workpiece geometric error on contact area, A_C

Considering

$$MRR = a \times V \quad (3)$$

Where

- a Depth of cut, mm
- V Workpiece infeed rate, mm/s

Thus, Eq. (2) can be further rewritten as:

$$(a \times V)/(A_c \times WRP) = F_n / A_c - F_{th} \quad (4)$$

This equation further reveals the relation among actual depth of cut with feed speed and contact area. Fig. 2 shows the change in A_C resulting from a geometric error on the workpiece for a hypothetically stiff roller. In practice, the roller will usually be flexible and there will be flattening of the contact wheel. Based on the hardness of the contact wheel and the kind of the grinding belt backing, a theoretical model will be developed in this study. Preliminary tests made by

measuring the difference between the displacement of the contact wheel and the real motion of the robot have shown that the contact area varies with the change of contact wheel hardness, belt tension, and workpiece geometry.

4.2 Local curvature in flexible robotic grinding vs equivalent Diameter in conventional grinding

From Eq. (4), it is observed that the local curvature will significantly affect the grinding force. In order to consider the effect of the cutting action for the difference in curvature of the wheel and work in the contact region in the conventional grinding process, Hahn [1] related the difference of curvature of internal or external grinding to the surface grinding by considering an equivalent diameter. Due to the characteristic of the robotic grinding process, such as the flexible contact wheel, the flexible robot arm, and the complex geometry of the workpiece, the equivalent diameter cannot be used in this process. Instead the local curvature is introduced to consider the change of the contact area during the grinding process. A speed factor will be calculated based on the normalized local curvature. The robot speed is adjusted according to the speed factor for each process point. The maximum speed of the path will be determined by the process model, which will be discussed in detail in the next section.

4.3 Contact stiffness and deformation

Process modeling describes the relationship of grinding force and depth of cut. However, actual depth of cut is affected by the overall system deformation. Therefore overall system model needs to be considered while applying the process modeling into robotic process control. Fig. 3 illustrates the compliant nature of the overall flexible robotic grinding system. A description of the appropriate terms is given as:

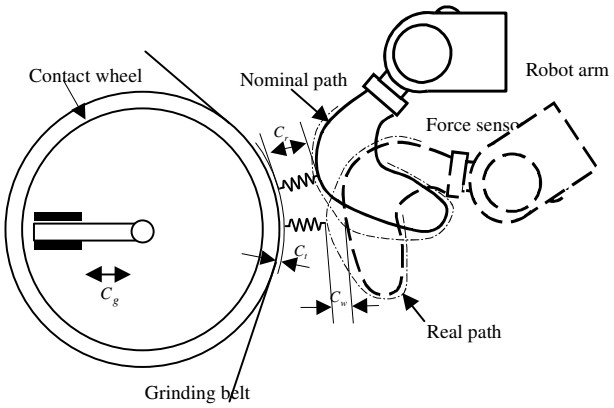

Fig. 3 Compliances in Robotic Belt Grinding

$$Robot\ compliance\ C_r = \frac{Robot\ deformation(\Delta x_r)}{Normal\ force(F_n)} \tag{5}$$

$$Grinding\ compliance\ C_w = \frac{Depth of\ cut(a)}{Normal\ force(F_n)} \tag{6}$$

$$Equivalent\ \ tooling\ \ compliance\ C_t = \frac{Toolwear(\Delta X_t)}{Normal\ force(F_n)} \tag{7}$$

$$Grinder\,Loop\,Compliance\ C_g = \frac{Grinder(\Delta X_g)}{Normal\ force(F_n)} \tag{8}$$

The total compliance between the workpiece and the grinding surface is formulated as:

$$C_{total} = \frac{\Delta X_{total}}{F_n} = \frac{\Delta X_r}{F_n} + \frac{a}{F_n} + \frac{\Delta X_t}{F_n} + \frac{\Delta X_g}{F_n} = C_r + C_w + C_t + C_g \tag{9}$$

It is obvious that when the normal force exists between the workpiece and the grinding tool, the deformations of the robot, the grinding wheel and the workpiece have to be considered if an accurate depth cut is obtained. The true depth of cut will be the total commanded displacement with subtraction of wheel deformation, robot arm deformation and wheel movement. Based on this fact, the process model in Eq. (4) will be rewritten as:

$$\frac{\left|\Delta X_{Total} - (C_r - C_t - C_g) \times F_n\right| \times V}{A_c \times WRP} = \frac{F_n}{A_c} - F_{th} \tag{10}$$

$$\frac{\Delta X_{Total} \cdot V}{A_c \cdot WRP} = (1 + \varepsilon \cdot V)\frac{F_n}{A_c} - F_{th} \tag{11}$$

where:

$$\varepsilon = \frac{(C_r + C_w + C_g)}{WRP} \tag{12}$$

and ΔX_{Total} is the robot commanded displacement, V is robot speed. This expression provides a robot control format for a flexible grinding process.

As shown in Fig. 4, a special experiment was performed to investigate deformation effects on the contact area. In this test, the robot arm holds the workpiece and pushes against the contact wheel. LVDT 1 and LVDT2 are used to measure the grinding wheel motion and the robot arm motion respectively. An ATI force/torque sensor is used to monitor the contact force. The belt tension pressure is 2 bars and the air cylinder pressure to support the contact wheel is 3.0 bars.

(9)

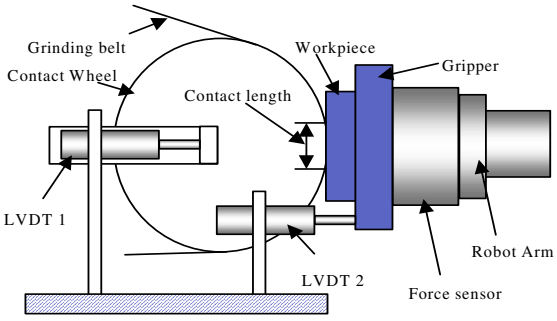

Fig. 4 Contact Area and Contact Stiffness Testing

Fig. 5 shows a clear picture of the robot compliance, wheel compliance and the grinding wheel and robot movement. It can be observed that the total command displacement has been divided into four portions: robot deformation, robot movement, grinding wheel deformation and grinding wheel movement.

As the robot approaches the grinding wheel, the force between the robot and the wheel will build up. Before the system reaches its critical stiffness, the robot and the grind wheel will be deformed due to the built-up force. The actual movement of the robot and the grinding wheel is smaller than the command displacement. When the system reaches the critical stiffness, the contact force is balanced with the air cylinder support pressure. At and after this critical point, the

contact force cannot increase any more and the robot moves as commanded. As for the contact wheel, the displacement keeps increasing until 2mm and then it will move with robot. Fig. 6 described the experimental results in terms of contact force. It can be seen that after the force reaches a certain point, the force will keep the constant, no matter how much the displacement is increased. All of the command displacement converts to the robot movement.

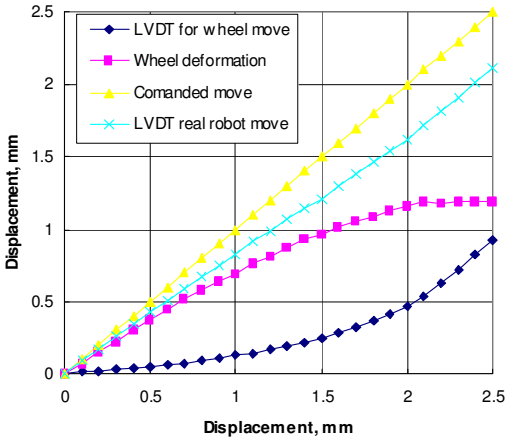

Fig. 5 Robot and Contact Wheel Deformation

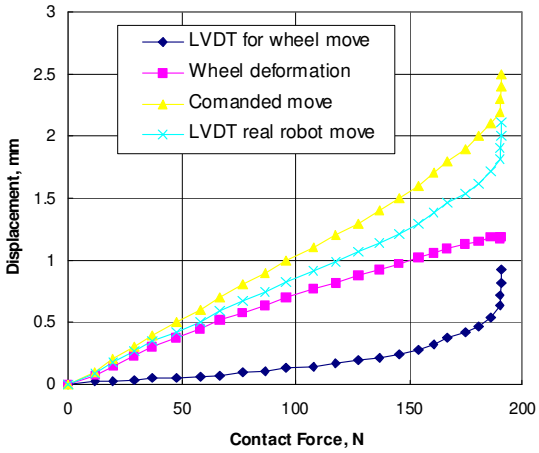

Fig. 6 Stiffness from Test Results

From Fig. 7, the following equation is used to calculate the contact length.

$$\left(\frac{L}{2}\right)^2 + (R-\Delta)^2 = R^2 \quad (13)$$

$$L = 2\sqrt{\Delta(2R-\Delta)} \approx 2\sqrt{2R\Delta} \quad (14)$$

R -- Contact wheel radius, mm

L -- Contact length, mm

θ -- Contact angle, degree

Δ -- Contact wheel deformation, mm

Combining the test results shown in Fig. 6 and using Eq. (14), the relationship between contact force and contact length can be plotted as shown in Fig. 8. This will be used in the process model to determine the contact area between the contact wheel and the workpiece under different contact force.

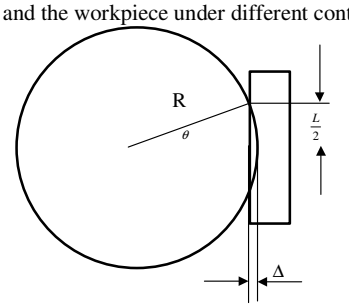

Fig. 7 Contact length calculation

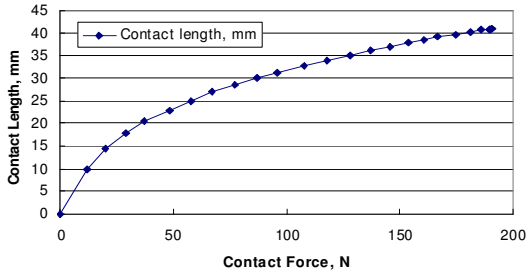

Fig. 8 Contact Length under Different Contact Force

5. PROCESS MODEL PARAMETER IDENTIFICATIONTS

The objective of all coated abrasive grinding is to produce the right MRR, dimension and finish in an acceptable period of time. A process model to predict the right operating condition is the key to achieve this goal. According to the analysis in the previous section, a series of experiments have been conducted to identify the model parameters. Table 1 shows the test parameters and their values.

Table 1. Test Parameters and their values

Test parameter	values
Contact Force	20N, 30N, 40N, 50 N
Belts type	• Norton #80, for 1st round material removal • Norton #120,for 2nd round material removal • Norton X65, for final polishing
Belt life	fresh, aging, old
Contact Wheels	• 50mm, Serrated, for material removal (L) • 30mm, plain, for final polishing (S)
Workpiece Speeds	20, 30, 40, 50, 60, 70, 80 mm/s
Belt Speeds	1500, 1600, 1700, 1800 rpm
Workpiece Material	B50A947A4

5.1 Test device setup

Fig.9 shows the setup for the process modeling test. An ABB IRB 4400-45 robot is used for the grinding process. A three-directional force/torque sensor from ATI is mounted between the workpiece gripper and the robot mounting plate to measure

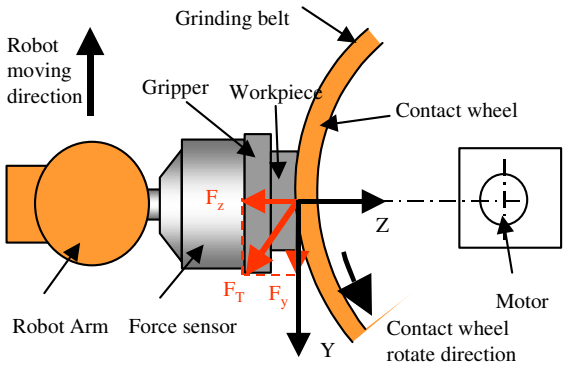

Fig. 9 Process Modeling Testing Setup

the contact force between the workpiece and the grinding belt.

5.2 Process model testing results

In this section, the test results for the Material Removal Rate under different operating conditions are illustrated. The test results include the MRR under different:

- Contact forces between workpiece and contact wheel
- Belt life
- Belts type and grit size
- Belt speeds
- Contact wheels (Large and small, plain and serrated)

Fig. 10 shows the material removal under different contact force and robot speed (Feedrate).

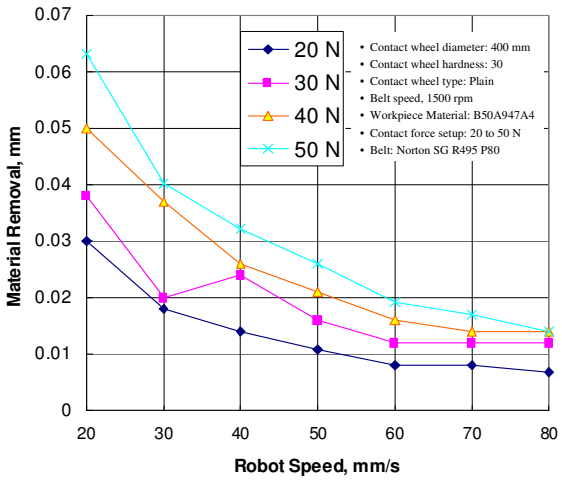

Fig. 10 Material removal under different contact force and robot speed

According to Eq. (3) and Eq. (4), if the grinding pressure keeps constant, then the relationship between the material removal (depth of cut) and the robot speed (feed rate) can be obtained as:

$$a \cdot V = \left(F_n - F_{th} \cdot A_c\right) \cdot WRP \tag{15}$$

If $\left(F_n - F_{th} \cdot A_c\right) \cdot WRP$ keeps constant, thus

$$a \times V = Const. \tag{16}$$

which is a hyperbola curve. With difference force set-up values, the hyperbola curve will change its position in the graphics. The experimental results shown in Fig. 10 prove the feasibility of model.

During this test, the lowest robot speed observed is higher than 20mm/s. Below this speed, the workpiece burn happened. On the other hand, the robot speed has to be limited under 50 mm/s to keep the reasonable material removal in production.

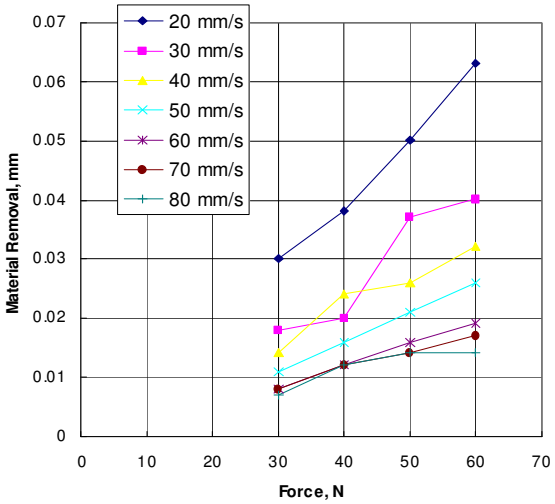

Fig.11. Threshold Force Under Different Robot Speed

From Eq. (2), the relationship between the material removal and the contact force is described by a linear equation, as shown in Fig 11. The threshold force F_{th} is the offset of this line equation, while WRP is the slope.

$$\frac{MRR}{WRP} = \frac{F_n}{A_C} - F_{th} \tag{17}$$

$$MRR = WRP\left(\frac{F_n}{A_c} - F_{th}\right) \tag{18}$$

Due to the additional flexibility of the belt grinding elements, it is anticipated that the threshold force behaviors considerably different from that of conventional grinding. This is because the extra flexibility will make the belt relatively sharper, which in turn increases WRP and further causes the reduction of the threshold force.

In grinding process, belt wear is another reason to cause the inconsistent workpiece finish. The common methods to compensate the belt wear include:

- Increase the contact force;
- Increase the belt speed;

Since increasing contact force will create more chance for the workpiece burn, the method of increasing belt speed is widely used. Fig. 12 shows that increasing the belt speed can increase the material removal effectively.

Belt types and grit size also affect WRP. To compare the performance of different belt types and grit sizes, both fresh belt (shown in Fig. 13) and the aging belt are tested. The Norton P80 and P120 are used to compare the same type of belts with different grit size. As can be seen, the material removal for fresh P80 and P120 belts does not make much difference. But the workpiece temperature will be much lower if using P80 rather than P120.

Fig 14 demonstrates the influence of the wheel size on the material removal rate. Under the same process condition, the smaller serrated contact wheel will produce a much larger

material removal rate than the large plain wheel. This is due to the larger pressure exerting on the smaller contact wheel if under the same force condition. However, when the belt becomes older, the difference in MRR caused by wheel size will be smaller. This can be explained by the reduction of the belt sharpness, as it will narrow the difference in the tangential cutting force.

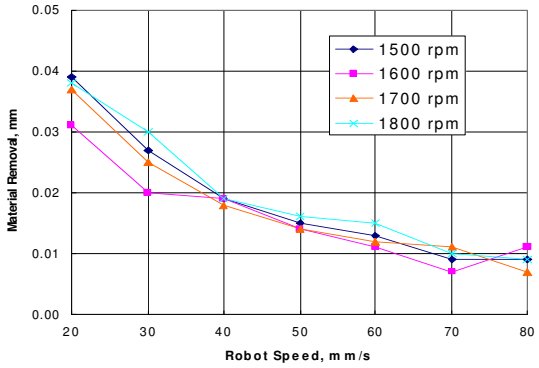

Fig. 12 Effect of Belt Speed on Material Removal

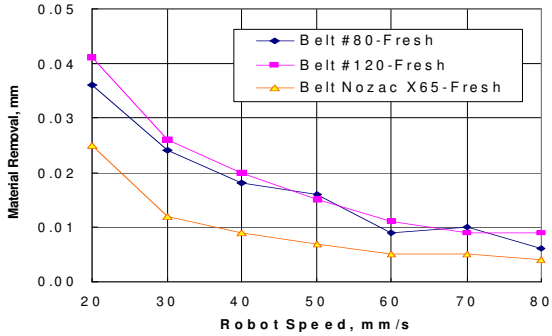

Fig. 13 Material Removal for Different Belts –Fresh

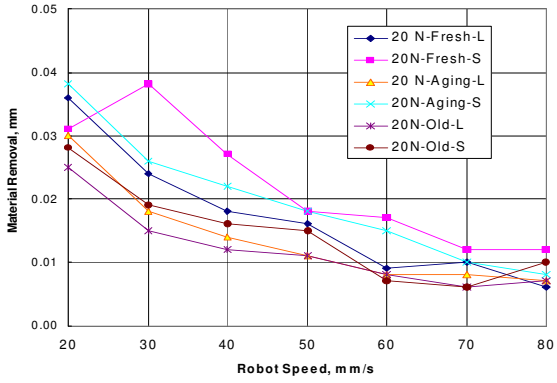

Fig. 14 Comparison of Different Contact Wheel

6. CONCLUSIONS

This paper proposes a new process model for flexible robotic grinding. Compared to 2D process model in conventional grinding, this new model provides a 3D relationship among force, MRR and contact area. According to this model, when contact area changes significantly in the grinding process, it becomes a variable in the process model, as opposed to being a constant in a conventional grinding model. Based on the new 3D model, a force/velocity control scheme has been proved effective for constant pressure control in flexible robotic grinding. Instead of using the equivalent diameter in conventional grinding for the contact area, the local curvature has been successfully introduced in this study to predict the workpiece infeed rate (robot speed).

Experimental result has verified that the validity of the new model for belt grinding. High quality and consistent workpieces have been finished by applying the proposed process model.

ACKNOWLEDGMENTS

The authors of this paper deeply appreciate Prof. Trevor Howes, for his advice during this study. Special thanks are also to Dr. Torgny Brogardh for his direction and support.

REFERENCES

[1] R. King and R. Hahn, *Handbook of Modern Grinding Technology*, Chapman and Hall, New York, London, 1986

[2] M. Her and H. Kazerooni, "Automated Robotic Deburring of Parts Using Compliance Control", *Journal of Dynamic System, Measurement, and Control, Transactions of the ASME*, Vol. 113, pp. 60-66, 1991

[3] D. Whitney and M. Brown, "Material Removal Model and Process Planning for Robot Grinding", *Conference Proceeding of 17th International Symposium on Industrial Robots*, Dearborn, Michigan, pp.19-29, 1987

[4] T.R. Kurfess, D. E. Whitney, and M. L. Broen, "Verification of a Dynamic Grinding Model", *Journal of Dynamic System, Measurement, and Control, Transactions of the ASME*, Vol. 110, pp. 403-409, 1988

[5] W. Persoons and P. Vanherck, "A Process Model for Robotic Cup Grinding", *Annals of the CIRP*, Vol. 42, No. 1, pp. 319, 1993